PHYSICAL REVIEW D **96,** 075025 (2017)

Solving the muon $g-2$ anomaly in deflected anomaly mediated SUSY breaking with messenger-matter interactions

Fei Wang,[1,*] Wenyu Wang,[2,†] and Jin Min Yang[3,4,‡]

[1]*School of Physics, Zhengzhou University, Zhengzhou 450000, People's Republic of China*
[2]*College of Applied Science, Beijing University of Technology, Beijing 100124, People's Republic of China*
[3]*CAS Key Laboratory of Theoretical Physics, Institute of Theoretical Physics, Chinese Academy of Sciences, Beijing 100190, People's Republic of China*
[4]*School of Physics, University of Chinese Academy of Sciences, Beijing 100049, People's Republic of China*

(Received 20 June 2017; published 18 October 2017)

We propose to introduce general messenger-matter interactions in the deflected anomaly mediated supersymmetry (SUSY) breaking (AMSB) scenario to explain the $g_\mu - 2$ anomaly. Scenarios with complete or incomplete grand unified theory (GUT) multiplet messengers are discussed, respectively. The introduction of incomplete GUT mulitiplets can be advantageous in various aspects. We found that the $g_\mu - 2$ anomaly can be solved in both scenarios under current constraints including the gluino mass bounds, while the scenarios with incomplete GUT representation messengers are more favored by the $g_\mu - 2$ data. We also found that the gluino is upper bounded by about 2.5 TeV (2.0 TeV) in scenario A and 3.0 TeV (2.7 TeV) in scenario B if the generalized deflected AMSB scenarios are used to fully account for the $g_\mu - 2$ anomaly at 3σ (2σ) level. Such a gluino should be accessible in the future LHC searches. Dark matter (DM) constraints, including DM relic density and direct detection bounds, favor scenario B with incomplete GUT multiplets. Much of the allowed parameter space for scenario B could be covered by the future DM direct detection experiments.

DOI: 10.1103/PhysRevD.96.075025

I. INTRODUCTION

Low energy supersymmetry (SUSY) is strongly motivated and regarded as one of the most appealing candidates for TeV-scale new physics beyond the standard model (SM). SUSY can not only solve the gauge hierarchy problem of the SM, but also elegantly explain the cosmic dark matter puzzle. Besides, the gauge coupling unification, which cannot be achieved in the SM, can be successfully realized in the framework of SUSY. Especially, the 125 GeV Higgs boson discovered by the LHC [1,2] lies miraculously in the narrow range of 115–135 GeV predicted by the minimal supersymmetric standard model (MSSM).

Although SUSY is an appealing extension of the SM, it seems to have some tensions with the current LHC data. In particular, no evidences of SUSY partners (sparticles) have been observed at the LHC. Actually, the LHC data has already set stringent constraints on sparticle masses [3,4] in simplified SUSY models, e.g., the gluino mass $m_{\tilde{g}} \gtrsim 1.9$ TeV for a massless lightest sparticle (LSP), the lightest stop mass $m_{\tilde{t}_1} \gtrsim 850$ GeV, and even stronger bounds on the first two generations of squarks. In fact, the LHC data agree quite well with the SM predictions and no significant deviations have been observed in flavor physics or electroweak precision measurements. So far the only sizable deviation comes from the so-called anomalous magnetic moment of the muon $a_\mu = (g_\mu - 2)/2$ measured by the E821 experiment at the Brookhaven National Laboratory [5], which shows a 3.2σ discrepancy from the SM prediction. The SUSY explanation of this anomaly requires relatively light sleptons and electroweak gauginos. If SUSY is indeed the new physics to explain all these experimental results, its spectrum must display an intricate structure. Therefore, the origin of SUSY breaking and its mediation mechanism, which determines the low energy SUSY spectrum, is a crucial issue.

There are many popular ways to mediate the SUSY breaking effects from the hidden sector to the visible MSSM sector, such as the gravity mediation [6], the gauge mediation [7], and the anomaly mediation [8] SUSY breaking (AMSB) mechanisms. The spectrum from the AMSB is insensitive to the ultraviolet (UV) theory [9] and automatically solves the SUSY flavor problem. Unfortunately, the AMSB scenario predicts tachyonic sleptons so that the minimal theory must be extended. There are several ways to tackle the tachyonic slepton problem [10]. A very elegant solution is the deflected AMSB [11] scenario, in which additional messenger sectors are introduced to deflect the renormalization group equation (RGE) trajectory and give new contributions to soft SUSY breaking terms [12–16].

*feiwang@zzu.edu.cn
†wywang@mail.itp.ac.cn
‡jmyang@itp.ac.cn

On the other hand, a relatively large number of messenger species are needed to give positive slepton masses with small negative deflection parameters. It is known that too many messenger fields may lead to strong gauge couplings below grand unified theory (GUT) scale or Landau pole below Planck scale. So it is preferred to introduce less messenger species to deflect the RGE trajectory and at the same time give positive slepton masses. In our previous work [17], we proposed to solve this problem by introducing general messenger-matter interactions in the deflected AMSB, which has advantages in several aspects.

Note that in order to preserve gauge coupling unification, the messenger species are generally fitted into complete representations of the GUT group. However, sometimes it is economic and well motivated to introduce incomplete representations of the GUT group, such as the $SU(3)_c$ and $SU(2)_L$ adjoint messengers in gauge mediated SUSY breaking [18–20]. The introduction of incomplete representations of messengers, which seems to spoil successful gauge coupling unification, can be natural in AMSB. This is due to the "decoupling theorem" in the ordinary anomaly mediation scenario, which states that the simple messenger threshold (by pure mass term) will not deflect the AMSB trajectory. By assigning a different origin for messenger thresholds [determined by moduli vacuum expectation value (VEV) or pure mass term], even a complete GUT group representation at high energy may seem as incomplete in AMSB at low energy. Therefore, the messengers in incomplete GUT representations should also be considered in the study of deflected AMSB.

In this work, we propose to study a generalized deflected AMSB scenario involving messenger-matter interactions with incomplete GUT multiplets. As noted before, the introduction of incomplete GUT mulitiplets in anomaly-type mediation scenarios can be advantageous in various aspects. Besides, virtues of ordinary deflected AMSB are kept while the undesirable Landau-pole-type problems can be evaded. Such scenarios can be preferable in solving the muon $g-2$ anomaly. It is known that a SUSY spectrum with heavy colored sparticles and light noncolored sparticles is needed in order to solve the muon $g-2$ anomaly and at the same time be compatible with the LHC data. We try to realize such a spectrum in the deflected AMSB scenario with general messenger-matter interactions, where the messengers can form complete or incomplete GUT representations. In our scenario, the slepton sector can receive additional contributions from both the messenger-matter interactions and ordinary deflected anomaly mediation to avoid tachyonic slepton masses, while the colored sparticles can be heavy to evade various collider constraints.

This paper is organized as follows. In Sec. II, we study the soft parameters in the deflected AMSB scenarios with different messenger-matter interactions. The explanation of the muon $g-2$ in our scenarios and the relevant numerical results are presented in Secs. III and IV contains our conclusions.

II. GENERAL MATTER-MESSENGER INTERACTIONS IN DEFLECTED AMSB

It is well known that the ordinary AMSB is bothered with the tachyonic slepton problem. The deflected AMSB scenario, which can change the RGE trajectory below the messenger thresholds, can elegantly solve such a problem. However, possible strong couplings at the GUT scale or the Landau-pole problem may arise with a small negative deflection parameter. Positively deflected AMSB, which may need specific forms of moduli superpotential [12] or strong couplings [21], could be favored in certain circumstances. However, our previous study indicated that the Landau-pole problem may still persist with a small positive deflection parameter in order to solve the $g_\mu-2$ anomaly.

In [17], we proposed to introduce general messenger-matter interactions in the messenger sector, which can have several advantages. In this work, the scenarios with complete or incomplete GUT representation messengers accompanied by messenger-matter interactions are studied. Note that the introduction of both adjoint messengers in **3** and **8** representations of $SU(2)_L$ and $SU(3)_c$, respectively, does not spoil the gauge coupling unification [18].

Besides, even if the low energy messenger sector seems to spoil the gauge coupling unification, the UV theory can still be consistent with the GUT requirement. As noted previously, the decoupling theorem in anomaly mediation ensures that the vectorlike thresholds with pure mass terms $M_T > M_{\rm mess}$ do not affect the AMSB trajectory upon messenger scales. So each low energy (deflected) AMSB theory with incomplete GUT multiplet messengers below messenger scale $M_{\rm mess}$ could be UV completed to a high energy theory with completed GUT multiplets at a certain scale upon $M_{\rm mess}$. Incomplete GUT multiplet messengers can also originate from orbifold GUT models by proper boundary conditions.

The formulas in deflected AMSB with messenger-matter interactions can be obtained from the wave function renormalization approach [22] with superfield wave function

$$\begin{aligned}\mathcal{Z}(\tilde{\mu};\tilde{X},\tilde{X}^\dagger) = Z(\mu;X,X^\dagger) &+ \left[\theta^2 F\frac{\partial}{\partial X}+\bar{\theta}^2F^\dagger\frac{\partial}{\partial X^\dagger}\right.\\ &\left.+(\theta^2\tilde{F}+\bar{\theta}^2\tilde{F}^\dagger)\frac{\partial}{\partial\mu}\right]Z(\mu;X,X^\dagger)\\ &+\theta^2\bar{\theta}^2\left(F^\dagger F\frac{\partial^2}{\partial X\partial X^\dagger}+F^\dagger\tilde{F}\frac{\partial^2}{\partial X^\dagger\partial\mu}\right.\\ &\left.+\tilde{F}^\dagger F\frac{\partial^2}{\partial X\partial\mu}+\tilde{F}^\dagger\tilde{F}\frac{\partial^2}{\partial\mu^2}\right)Z(\mu;X,X^\dagger).\end{aligned}$$

After canonically normalizing the field,

$$Q'\equiv Z^{1/2}\left[1+\theta^2\left(\frac{F}{M}\frac{\partial}{\partial\ln X}+\frac{\tilde{F}}{\mu}\frac{\partial}{\partial\ln\mu}\right)\ln Z(\mu;X,X^\dagger)\right], \tag{2.1}$$

we can obtain the sfermion masses for the most general forms of deflected AMSB,

$$m^2 = -\left[\left(\frac{F}{M}\right)^2 \frac{\partial^2}{\partial \ln X^\dagger \partial \ln X} + \left(\frac{\tilde{F}}{\mu}\right)^2 \frac{\partial^2}{\partial \ln \mu^2} + \frac{F\tilde{F}}{M\mu}\left(\frac{\partial^2}{\partial \ln X^\dagger \partial \ln \mu} + \frac{\partial^2}{\partial \ln X \partial \ln \mu}\right)\right] \ln Z(\mu; X, X^\dagger). \tag{2.2}$$

From the canonicalized normalized superpotential

$$\mathcal{L} = \int d^2\theta \sum_{i=a,b,c} \left[1 - \theta^2\left(F\frac{\partial}{\partial X} + \tilde{F}\frac{\partial}{\partial \mu}\right) \ln Z(\mu; X, X^\dagger)\right] \times (Z^{-1/2}Q_i') \frac{\partial W[(Z^{-1/2}Q_i')]}{\partial (Z^{-1/2}Q_i')},$$

we can obtain the trilinear soft terms

$$\frac{A_{abc}}{y_{abc}} = \sum_{i=a,b,c} \left(\frac{F}{M}\frac{\partial}{\partial X} + \frac{\tilde{F}}{\mu}\frac{\partial}{\partial \mu}\right) \ln Z_i(\mu; X, X^\dagger). \tag{2.3}$$

In our scenario, we have the following replacement:

$$\frac{F}{M} \to dF_\phi, \qquad \frac{\tilde{F}}{\mu} \to -F_\phi/2. \tag{2.4}$$

Details on general messenger-matter interactions in deflected AMSB can be found in our previous work [17].

A. Two scenarios with messenger-matter interactions

(i) Scenario A: deflected AMSB with complete SU(5) GUT representations messengers.

We introduce the following N family of new messengers that are fitted into a **5** and $\bar{\mathbf{5}}$ representation of SU(5) GUT group to deflect the AMSB trajectory

$$\bar{Q}^I_\phi(1,2)_{1/2}, \qquad \tilde{Q}^I_\phi(1,\bar{2})_{-1/2}, \qquad \bar{T}^I_\phi(\bar{3},1)_{1/3}, \qquad T^I_\phi(3,1)_{-1/3}, \quad (I = 1,\ldots,N).$$

We introduce the following superpotential that involves messenger-MSSM-MSSM interaction, typically the slepton-slepton-messenger interaction,

$$W = \sum_I (\lambda_A S \bar{Q}^I_\phi \tilde{Q}^I_\phi + \lambda_B S \bar{T}^I_\phi T^I_\phi) + \lambda_X S \bar{Q}^A_\phi \tilde{H}_d + W(S) + \sum_{i,j}[\tilde{y}^E_{ij} L_{L,i} \tilde{Q}^A_\phi E^c_{L,j} + \tilde{y}^D_{ij} Q_{L,i} \tilde{H}_d D^c_{L,j} + y^U_{ij} Q_{L,i} H_u U^c_{L,j}], \tag{2.5}$$

with a certain form of superpotential $W(S)$ for pseudomoduli field S to determine the deflection parameter d. From the form of the interaction, we can see that the slepton soft SUSY breaking parameters will be different from the ordinary deflected AMSB results.

(ii) Scenario B: deflected AMSB with incomplete SU(5) GUT representations messengers.

Motivated by the gauge mediated SUSY breaking with adjoint messenger scenario, we introduce the following incomplete SU(5) GUT representation messengers to deflect the AMSB trajectory:

$$\Sigma^I_O(8,1)_0, \qquad \sigma^I_T(1,3), \qquad Z^J(1,1)_1, \qquad \bar{Z}^J(1,1)_{-1}, \qquad I,J = (1,\ldots,M), \qquad \bar{Q}^A_\phi(1,2)_{1/2}, \qquad \tilde{Q}^A_\phi(1,\bar{2})_{-1/2}, \qquad \bar{T}^A_\phi(\bar{3},1)_{1/3}, \qquad T^A_\phi(3,1)_{-1/3}.$$

We note that additional singlet messengers Z^I with nontrivial $U(1)_Y$ quantum number can be introduced to deflected the $\tilde{E}^c_L$ slepton RGE trajectory. As in the previous scenario, the superpotential also involves messenger-MSSM-MSSM interaction, typically the slepton-slepton-messenger interaction,

$$W = \lambda_A S \bar{Q}^A_\phi \tilde{Q}^A_\phi + \lambda_B S \bar{T}^A_\phi T^A_\phi + \sum_I [\lambda_O S \mathrm{Tr}(\Sigma^I_O \Sigma^I_O) + \lambda_T S \mathrm{Tr}(\Sigma^I_T \Sigma^I_T) + \lambda_Z S \bar{Z}^I Z^I] + \lambda_X S \bar{Q}^A_\phi \tilde{H}_d + \sum_{i,j}[\tilde{y}^E_{ij} L_{L,i} \tilde{Q}^A_\phi E^c_{L,j} + \tilde{y}^D_{ij} Q_{L,i} \tilde{H}_d D^c_{L,j} + y^U_{ij} Q_{L,i} H_u U^c_{L,j}] + W(S). \tag{2.6}$$

We can see that there will be mixing between the messenger $\tilde{Q}^A_\phi$ and $\tilde{H}_d$ (as well as Q^B_ϕ and H_u). We define the new states

$$Q^A_\phi \equiv \frac{\lambda_A \tilde{Q}^A_\phi + \lambda_X \tilde{H}_d}{\sqrt{\lambda_A^2 + \lambda_X^2}}, \qquad H_d \equiv \frac{-\lambda_X \tilde{Q}^A_\phi + \lambda_A \tilde{H}_d}{\sqrt{\lambda_A^2 + \lambda_X^2}}. \tag{2.7}$$

After the substitution of the new states, the superpotential changes to

$$W = \sqrt{\lambda_A^2 + \lambda_X^2} S \bar{Q}^A_\phi Q^A_\phi + \sum_{i,j} y^U_{ij} Q_{L,i} H_u U^c_{L,j} + \sum_{F_H = T^I_\phi, Q^I_\phi, \cdots} \lambda_{F_H} S \bar{F}_H F_H + W(S) + \sum_{i,j} \tilde{y}^E_{ij} L_{L,i} \frac{\lambda_A Q^A_\phi - \lambda_X H_d}{\sqrt{\lambda_A^2 + \lambda_X^2}} E^c_{L,j} + \tilde{y}^D_{ij} Q_{L,i} \frac{\lambda_X Q^A_\phi + \lambda_A H_d}{\sqrt{\lambda_A^2 + \lambda_X^2}} D^c_{L,j}. \tag{2.8}$$

We have the following relation:

$$\tilde{y}^E_{ij}\frac{\lambda_X}{\sqrt{\lambda_A^2+\lambda_X^2}}=y^E_{ij},\qquad -\tilde{y}^D_{ij}\frac{\lambda_A}{\sqrt{\lambda_A^2+\lambda_X^2}}=y^D_{ij}. \tag{2.9}$$

We define

$$\tilde{y}^E_{ij}\frac{\lambda_A}{\sqrt{\lambda_A^2+\lambda_X^2}}\equiv-\lambda^E_{ij},\qquad -\tilde{y}^D_{ij}\frac{\lambda_X}{\sqrt{\lambda_A^2+\lambda_X^2}}\equiv\lambda^D_{ij},$$
$$\sqrt{\lambda_A^2+\lambda_X^2}\equiv\lambda_S. \tag{2.10}$$

So the superpotential can be rewritten as

$$\begin{aligned}W=&\lambda_S S\bar{Q}^A_\phi Q^A_\phi+\sum_{i,j}y^U_{ij}Q_{L,i}H_uU^c_{L,j}\\&+\sum_{F_H=Z^I,Q^I,\cdots}\lambda_{F_H}S\bar{F}_HF_H+W(S)\\&-\sum_{i,j}[\lambda^E_{ij}L_{L,i}Q^A_\phi E^c_{L,j}+y^E_{ij}L_{L,i}H_dE^c_{L,j}\\&+\lambda^D_{ij}Q_{L,i}Q^A_\phi D^c_{L,j}+y^D_{ij}Q_{L,i}H_dD^c_{L,j}].\end{aligned} \tag{2.11}$$

For simplicity, we chose $\lambda^E_{ij}=\lambda_E\delta_{ij}$, $\lambda^D_{ij}=\lambda_D\delta_{ij}$ to be diagonal. Below the messenger threshold determined by the VEV of pseudomoduli S, we can integrate out the heavy fields F_H, Q^A_ϕ and obtain the low energy MSSM.

B. The soft SUSY spectrum in two scenarios

From the superpotential, the soft SUSY breaking parameters can be calculated. In the calculation, the wave function renormalization approach [23] is used in which messenger threshold $M^2_{\rm mess}$ is replaced by spurious chiral fields X with $M^2_{\rm mess}=X^\dagger X$. The most general type of expressions in AMSB can be found in our previous work [17].

We can calculate the change of the gauge beta function

$$\Delta\beta_{g_i}=\frac{1}{16\pi^2}g_i^3\Delta b_{g_i}, \tag{2.12}$$

with

$$\Delta(b_3,b_2,b_1)=(N,N,N), \tag{2.13}$$

for scenario A. For scenario B we consider two cases. One is

$$\Delta(b_3,b_2,b_1)=(3M+1,2M+1,1)\ \ \text{scenario B1}, \tag{2.14}$$

in which $'I=M,J=0'$ is adopted to guarantee apparently gauge coupling unification. The other is

$$\Delta(b_3,b_2,b_1)=\left(3M+1,2M+1,\frac{6M}{5}+1\right)\ \ \text{scenario B2}, \tag{2.15}$$

with $'I=J=M'$ in which apparently the gauge coupling unification is spoiled. However, as we discussed previously, successful GUT may still be possible if certain additional incomplete messengers upon the X threshold determined by pure mass terms are introduced in the UV completed theory.

From the general expressions in Eq. (2.2), we can see that there are three types of contributions to the soft SUSY breaking parameters:

(i) The interference contribution part given by

$$\begin{aligned}\delta^I&=\frac{\partial^2}{\partial\ln\mu\partial\ln X}\ln Z^D_{ab}\\&=\frac{\partial^2}{\partial\ln\mu\partial\ln X}Z^D-\frac{\partial}{\partial\ln\mu}Z^D\frac{\partial}{\partial\ln X}Z^D\\&=\left(\frac{\Delta G^D_a}{2}\frac{\partial}{\partial Z^D_a}+\frac{\Delta\beta_{g_r}}{2}\frac{\partial}{\partial g_r}\right)G^- -G^D_a\frac{\Delta G_a}{2}.\end{aligned} \tag{2.16}$$

In our convention, the anomalous dimensions are expressed in the holomorphic basis [24,25]

$$\begin{aligned}G^i&\equiv\frac{dZ_{ij}}{d\ln\mu}\\&\equiv-\frac{1}{8\pi^2}\left(\frac{1}{2}d^i_{kl}\lambda^*_{ikl}\lambda_{jmn}Z^{-1*}_{\rm km}Z^{-1*}_{ln}-2c^i_rZ_{ij}g_r^2\right).\end{aligned} \tag{2.17}$$

We define $(\Delta G\equiv G^+-G^-)$ the discontinuity across the integrated heavy field threshold with $G^+(G^-)$ denoting the value upon (below) such a threshold, respectively.

The discontinuities of the relevant couplings are given as

$$\Delta G_{y_t}=-\frac{1}{8\pi^2}(\lambda_D^2), \tag{2.18}$$

$$\Delta G_{y_b}=-\frac{1}{8\pi^2}(3\lambda_D^2), \tag{2.19}$$

$$\Delta G_{y_\tau}=-\frac{1}{8\pi^2}(3\lambda_E^2). \tag{2.20}$$

We take into account the terms involving $y_t,y_b,y_\tau,g_i,\lambda$, and the subleading terms are neglected in the calculation. The new interference contributions from the messenger-matter interactions are given as

$$2\delta^I_{Q_{L,i}} = \delta_{i,3}\frac{dF_\phi^2}{8\pi^2}[y_t^2\Delta G_{y_t} + y_b^2\Delta G_{y_b}], \quad (2.21)$$

$$2\delta^I_{U^c_{L,i}} = \delta_{i,3}\frac{dF_\phi^2}{8\pi^2}[2y_t^2\Delta G_{y_t}], \quad (2.22)$$

$$2\delta^I_{D^c_{L,i}} = \delta_{i,3}\frac{dF_\phi^2}{8\pi^2}[2y_b^2\Delta G_{y_b}], \quad (2.23)$$

$$2\delta^I_{L_{L,i}} = \delta_{i,3}\frac{dF_\phi^2}{8\pi^2}[y_\tau^2\Delta G_{y_\tau}], \quad (2.24)$$

$$2\delta^I_{E^c_{L,i}} = \delta_{i,3}\frac{dF_\phi^2}{8\pi^2}[2y_\tau^2\Delta G_{y_\tau}], \quad (2.25)$$

$$2\delta^I_{H_u} = \frac{dF_\phi^2}{8\pi^2}[3y_t^2\Delta G_{y_t}], \quad (2.26)$$

$$2\delta^I_{H_d} = \frac{dF_\phi^2}{8\pi^2}[3y_b^2\Delta G_{y_b} + y_\tau^2\Delta G_{y_\tau}], \quad (2.27)$$

with $\delta_{i,j}$ being the Kronecker delta. Terms involving the gauge parts are absorbed in the deflected AMSB contributions involving G_i.

(ii) The pure gauge mediation part given by

$$\delta^G = \frac{\partial^2}{\partial \ln X \ln X^\dagger}\ln Z^D = \frac{\partial^2}{\partial \ln X \ln X^\dagger}Z^D - \frac{\partial Z^D}{\partial \ln X}\frac{\partial Z^D}{\partial \ln X^\dagger}. \quad (2.28)$$

Note that

$$\Delta G_{Q_iQ_i} = -\frac{1}{8\pi^2}[\lambda_D^2], \quad (2.29)$$

$$\Delta G_{D_iD_i} = -\frac{1}{8\pi^2}[2\lambda_D^2], \quad (2.30)$$

$$\Delta G_{E_iE_i} = -\frac{1}{8\pi^2}2\lambda_E^2, \quad (2.31)$$

$$\Delta G_{L_iL_i} = -\frac{1}{8\pi^2}\lambda_E^2, \quad (2.32)$$

and

$$G^+_{L_iL_i} = -\frac{1}{8\pi^2}[\lambda_E^2 + y_\tau^2\delta_{i,3}], \quad (2.33)$$

$$G^+_{E_iE_i} = -\frac{1}{8\pi^2}2[\lambda_E^2 + y_\tau^2\delta_{i,3}], \quad (2.34)$$

$$G^+_{Q_iQ_i} = -\frac{1}{8\pi^2}[\lambda_D^2 + (y_b^2 + y_t^2)\delta_{i,3}], \quad (2.35)$$

$$G^+_{D_iD_i} = -\frac{1}{8\pi^2}2[\lambda_D^2 + y_b^2\delta_{i,3}], \quad (2.36)$$

$$G^+_{Q_\phi Q_\phi} = -\frac{1}{8\pi^2}[\lambda_E^2 + 3\lambda_D^2 + \lambda_S^2], \quad (2.37)$$

and also the anomalous dimension above the messenger threshold

$$G^+_{\lambda^D_{ii}} = G^+_{Q_iQ_i} + G^+_{D_iD_i} + G^+_{Q_\phi Q_\phi} = -\frac{1}{8\pi^2}\left[6\lambda_D^2 + \lambda_E^2 + \lambda_S^2 + (3y_b^2 + y_t^2)\delta_{i,3} - \frac{16}{3}g_3^2 - 3g_2^2 - \frac{7}{15}g_1^2\right], \quad (2.38)$$

$$G^+_{\lambda^E_{ii}} = G^+_{L_iL_i} + G^+_{E_iE_i} + G^+_{Q_\phi Q_\phi} = -\frac{1}{8\pi^2}\left[4\lambda_E^2 + 3\lambda_D^2 + \lambda_S^2 + 3y_\tau^2\delta_{i,3} - 3g_2^2 - \frac{9}{5}g_1^2\right], \quad (2.39)$$

so we have

$$4\delta^G_{Q_i} = \frac{d^2F_\phi^2}{8\pi^2}[\lambda_D^2 G^+_{\lambda^D_{ii}}] - \frac{d^2F_\phi^2}{8\pi^2}\delta_{i,3}[y_t^2\Delta G_{y_t} + y_b^2\Delta G_{y_b}], \quad (2.40)$$

$$4\delta^G_{D_i} = \frac{d^2F_\phi^2}{8\pi^2}[2\lambda_D^2 G^+_{\lambda^D_{ii}}] - \frac{d^2F_\phi^2}{8\pi^2}\delta_{i,3}[2y_b^2\Delta G_{y_b}], \quad (2.41)$$

$$4\delta^G_{U_i} = -\frac{d^2F_\phi^2}{8\pi^2}\delta_{i,3}[2y_t^2\Delta G_{y_t}], \quad (2.42)$$

$$4\delta^G_{L_i} = \frac{d^2F_\phi^2}{8\pi^2}[\lambda_E^2 G^+_{\lambda^E_{ii}}] - \frac{d^2F_\phi^2}{8\pi^2}\delta_{i,3}[y_\tau^2\Delta G_{y_\tau}], \quad (2.43)$$

$$4\delta^G_{E_i} = \frac{d^2F_\phi^2}{8\pi^2}[2\lambda_E^2 G^+_{\lambda^E_{ii}}] - \frac{d^2F_\phi^2}{8\pi^2}\delta_{i,3}[2y_\tau^2\Delta G_{y_\tau}], \quad (2.44)$$

$$4\delta^G_{H_u} = -\frac{d^2F_\phi^2}{8\pi^2}[3y_t^2\Delta G_{y_t}], \quad (2.45)$$

$$4\delta^G_{H_d} = -\frac{d^2F_\phi^2}{8\pi^2}[3y_b^2\Delta G_{y_b} + y_\tau^2\Delta G_{y_\tau}]. \quad (2.46)$$

(iii) The pure deflected AMSB contributions without messenger-matter interactions given by

$$\delta_A = \frac{d^2Z^D}{dt^2} - \left(\frac{dZ^D}{dt}\right)^2 = \left(G_a^D\frac{\partial}{\partial Z_a} + \beta_g^i\frac{\partial}{\partial g_i}\right)G^D - (G_D^2). \quad (2.47)$$

The expressions are given by

$$\delta^A_{\tilde{Q}_{L,i}} = \frac{F_\phi^2}{16\pi^2}\left[\frac{8}{3}G_3\alpha_3^2 + \frac{3}{2}G_2\alpha_2^2 + \frac{1}{30}G_1\alpha_1^2\right] + \delta_{3,i}\frac{F_\phi^2}{(16\pi^2)^2}y_t^2\left(6y_t^2 + y_b^2 - \frac{16}{3}g_3^2 - 3g_2^2 - \frac{13}{15}g_1^2\right) + \delta_{3,i}\frac{F_\phi^2}{(16\pi^2)^2}y_b^2\left(y_t^2 + 6y_b^2 + y_\tau^2 - \frac{16}{3}g_3^2 - 3g_2^2 - \frac{7}{15}g_1^2\right), \tag{2.48}$$

$$\delta^A_{\tilde{U}^c_{L,i}} = \frac{F_\phi^2}{16\pi^2}\left[\frac{8}{3}G_3\alpha_3^2 + \frac{8}{15}G_1\alpha_1^2\right] + \delta_{3,i}\frac{F_\phi^2}{(16\pi^2)^2}2y_t^2\left(6y_t^2 + y_b^2 - \frac{16}{3}g_3^2 - 3g_2^2 - \frac{13}{15}g_1^2\right),$$
$$\delta^A_{\tilde{D}^c_{L,i}} = \frac{F_\phi^2}{16\pi^2}\left[\frac{8}{3}G_3\alpha_3^2 + \frac{2}{15}G_1\alpha_1^2\right] + \delta_{3,i}\frac{F_\phi^2}{(16\pi^2)^2}2y_b^2\left(y_t^2 + 6y_b^2 + y_\tau^2 - \frac{16}{3}g_3^2 - 3g_2^2 - \frac{7}{15}g_1^2\right), \tag{2.49}$$

$$\delta^A_{\tilde{H}_u} = \frac{F_\phi^2}{16\pi^2}\left[\frac{3}{2}G_2\alpha_2^2 + \frac{3}{10}G_1\alpha_1^2\right] + \frac{F_\phi^2}{(16\pi^2)^2}3y_t^2\left(6y_t^2 + y_b^2 - \frac{16}{3}g_3^2 - 3g_2^2 - \frac{13}{15}g_1^2\right), \tag{2.50}$$

$$\delta^A_{\tilde{H}_d} = \frac{F_\phi^2}{16\pi^2}\left[\frac{3}{2}G_2\alpha_2^2 + \frac{3}{10}G_1\alpha_1^2\right] + \frac{F_\phi^2}{(16\pi^2)^2}3y_b^2\left(y_t^2 + 6y_b^2 + y_\tau^2 - \frac{16}{3}g_3^2 - 3g_2^2 - \frac{7}{15}g_1^2\right) + \frac{F_\phi^2}{(16\pi^2)^2}y_\tau^2\left(4y_\tau^2 + 3y_b^2 - 3g_2^2 - \frac{9}{5}g_1^2\right), \tag{2.51}$$

$$\delta^A_{\tilde{L}_{L,i}} = \frac{F_\phi^2}{16\pi^2}\left[\frac{3}{2}G_2\alpha_2^2 + \frac{3}{10}G_1\alpha_1^2\right] + \delta_{3,i}\frac{F_\phi^2}{(16\pi^2)^2}y_\tau^2\left(4y_\tau^2 + 3y_b^2 - 3g_2^2 - \frac{9}{5}g_1^2\right), \tag{2.52}$$

$$\delta^A_{\tilde{E}^c_{L,i}} = \frac{F_\phi^2}{16\pi^2}\left[\frac{6}{5}G_1\alpha_1^2\right] + \delta_{3,i}\frac{F_\phi^2}{(16\pi^2)^2}2y_\tau^2\left(4y_\tau^2 + 3y_b^2 - 3g_2^2 - \frac{9}{5}g_1^2\right), \tag{2.53}$$

with

$$G_i = (\Delta b_i)d^2 + 2(\Delta b_i)d - b_i, \tag{2.54}$$

$$(b_1, b_2, b_3) = \left(\frac{33}{5}, 1, -3\right). \tag{2.55}$$

So we obtain the final results of soft SUSY breaking parameters for sfermions

$$m_i^2 = -\delta_i^I + \delta_i^G + \delta_i^A, \tag{2.56}$$

with $'d'$ being the deflection parameter.

The trilinear coupling also receives new contributions, which are given by

$$A_t = \frac{F_\phi}{16\pi^2}\left[6y_t^2 + y_b^2 - (\lambda_D^2)d - \frac{16}{3}g_3^2 - 3g_2^2 - \frac{13}{15}g_1^2\right], \tag{2.57}$$

$$A_b = \frac{F_\phi}{16\pi^2}\left[y_t^2 + 6y_b^2 + y_\tau^2 - (3\lambda_D^2)d - \frac{16}{3}g_3^2 - 3g_2^2 - \frac{7}{15}g_1^2\right], \tag{2.58}$$

$$A_\tau = \frac{F_\phi}{16\pi^2}\left[4y_\tau^2 + 3y_b^2 - (3\lambda_E^2)d - 3g_2^2 - \frac{9}{5}g_1^2\right], \tag{2.59}$$

$$A_{U;1,2} = \frac{F_\phi}{16\pi^2}\left[-(\lambda_D^2)d - \frac{16}{3}g_3^2 - 3g_2^2 - \frac{13}{15}g_1^2\right], \tag{2.60}$$

$$A_{D;1,2} = \frac{F_\phi}{16\pi^2}\left[-(3\lambda_D^2)d - \frac{16}{3}g_3^2 - 3g_2^2 - \frac{7}{15}g_1^2\right], \tag{2.61}$$

$$A_{E;1,2} = \frac{F_\phi}{16\pi^2}\left[-(3\lambda_E^2)d - 3g_2^2 - \frac{9}{5}g_1^2\right]. \tag{2.62}$$

The gaugino masses are determined by

$$m_{\lambda_i} = g^2\frac{F_\phi}{2}\left(\frac{\partial}{\partial \ln \mu} - d\frac{\partial}{\partial \ln |X|}\right)\frac{1}{g^2(\mu, X)} = g^2\frac{F_\phi}{2}\left(2\frac{1}{16\pi^2}b_i - 2d\frac{1}{16\pi^2}\Delta b_i\right) = g^2\frac{F_\phi}{16\pi^2}(b_i - d\Delta b_i). \tag{2.63}$$

So we have

$$m_{\lambda_i} = \frac{F_\phi}{4\pi}\alpha_i(b_i - d\Delta b_i). \tag{2.64}$$

Therefore, the gaugino masses at the messenger scale are given as

$$M_3 = \frac{F_\phi}{4\pi}\alpha_3[-3 - d(\Delta b_3)], \tag{2.65}$$

$$M_2 = \frac{F_\phi}{4\pi}\alpha_2[1 - d(\Delta b_2)], \tag{2.66}$$

$$M_1 = \frac{F_\phi}{4\pi}\alpha_1[6.6 - d(\Delta b_1)]. \tag{2.67}$$

It is well known in AMSB that naively adding a supersymmetric μ term to the Lagrangian leads to unrealistically large $B\mu = \mu F_\phi$. So the generations of μ and B_μ in AMSB may have a different origin and are model dependent. In fact, there are already many proposals to generate realistic μ and $B\mu$, for example, by promoting to NMSSM [26] or introducing a new singlet [27]. We treat them as free parameters in this scenario.

III. SOLVING THE MUON $g-2$ ANOMALY IN OUR SCENARIO

The E821 experimental result of the muon anomalous magnetic moment at the Brookhaven AGS [28]

$$a_\mu^{\text{expt}} = 116592089(63) \times 10^{-11} \tag{3.1}$$

is larger than the SM prediction [29]

$$a_\mu^{\text{SM}} = 116591834(49) \times 10^{-11}. \tag{3.2}$$

The deviation is about 3.2σ,

$$\Delta a_\mu(\text{expt—SM}) = (255 \pm 80) \times 10^{-11}. \tag{3.3}$$

SUSY can yield sizable contributions to the muon $g-2$ that dominantly come from the chargino-sneutrino and the neutralino-smuon loop diagrams. The muon $g-2$ anomaly, which is order 10^{-9}, can be explained for $m_{\text{SUSY}} = \mathcal{O}(100)$ GeV and $\tan\beta = \mathcal{O}(10)$. In our scenario, slepton masses as well as M_1, M_2 can be relatively light. On the other hand, the colored sparticles can be heavy to evade possible constraints from the LHC, the SUSY flavor, and CP problems. Some recent discussions can be seen in [30].

The soft terms are characterized by the following free parameters at the messenger scale:

$$d, M_{\text{mess}}, F_\phi, \tan\beta, \lambda^D, \lambda^E, \lambda_S, \lambda_{F_H}. \tag{3.4}$$

All the inputs should be seen as the boundary conditions at the messenger scale, which after RGE running to the electroweak (EW) scale, could give the low energy spectrum. About these parameters, we have the following comments:

(i) The value of F_ϕ is chosen to lie in the range 1 TeV $< F_\phi <$ 500 TeV. We know that the value of F_ϕ determines the whole spectrum. On the one hand, F_ϕ cannot be very low due to the constraints from the gaugino masses. A very heavy F_ϕ spoils the electroweak symmetry breaking requirement and gives a Higgs mass heavier than the LHC results.

(ii) The messenger scale M_{mess} can be chosen to be less than the GUT scale and at the same time heavier than the sparticle spectrum. So we choose 1 TeV $\leq M_{\text{mess}} \leq 10^{15}$ GeV.

(iii) We choose the deflection parameter in the range $-5 \leq d \leq 5$ and $\tan\beta$ in the range $2 \leq \tan\beta \leq 50$.

(iv) The parameters $\lambda_D, \lambda_E, \cdots$ can be chosen in the range $0 < |\lambda| < \sqrt{4\pi}$, which ensures positive contributions to slepton masses regardless of the (sign of) deflection parameter d. This is the advantage of our scenario, which needs fewer messenger species with a given d.

We also take into account the following collider and dark matter (DM) constraints:

(1) The mass range for the Higgs boson 123 GeV $< M_h <$ 127 GeV from ATLAS and CMS [1,2].

(2) The lower bounds on neutralino and charginos masses, including the invisible decay bounds for the Z-boson [31].

(3) The dark matter relic density from the Planck result $\Omega_{\text{DM}} = 0.1199 \pm 0.0027$ [32] (in combination with the WMAP data [33]) and the limits of the LUX-2016 [34], the PandaX [35] spin-independent (SI) dark matter scattering cross section.

(4) Flavor constraints from the rare decays of B-mesons
(a) Constraints from $\text{Br}(B_s \to \mu^+\mu^-)$ [36]

$$1.6 \times 10^{-9} \leq \text{Br}(B_s \to \mu^+\mu^-) \leq 4.2 \times 10^{-9}\ (2\sigma), \tag{3.5}$$

(b) Constraints from $\text{Br}(B_S \to X_s\gamma)$ etc. [37]

$$2.99 \times 10^{-4} \leq \text{Br}(B_S \to X_s\gamma) < 3.87 \times 10^{-4}\ (2\sigma). \tag{3.6}$$

(5) The electroweak precision obsearvables [38], such as

$$\delta M_W^{\text{exp}} \approx \pm 30\ \text{MeV}, \qquad \delta \sin\theta_{\text{eff}}^{\text{exp}} \approx \pm 15 \times 10^{-5}. \tag{3.7}$$

(6) Current LHC constraints on sparticle masses [39]:
(i) Gluino mass $m_{\tilde{g}} \gtrsim 1.5 \sim 1.9$ TeV,
(ii) light stop mass $m_{\tilde{t}_1} \gtrsim 0.85$ TeV,

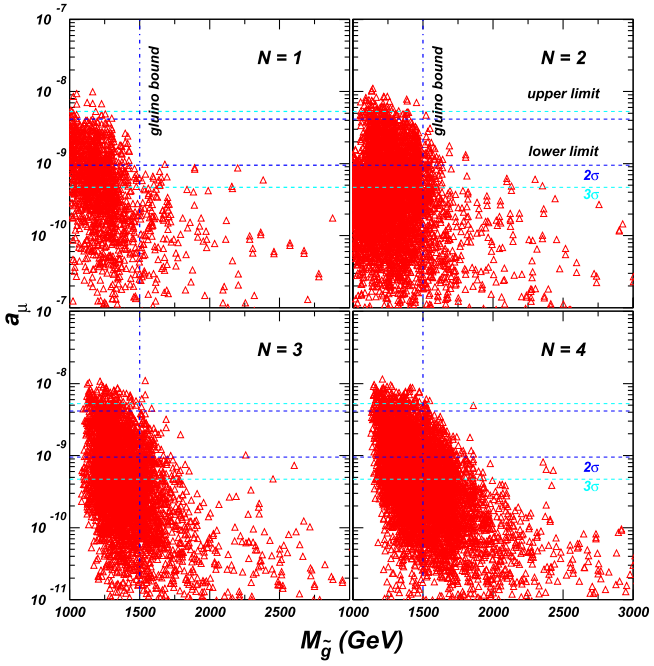

FIG. 1. The scatter plots of the surviving samples showing the muon $g-2$ versus the gluino mass in scenario A with complete GUT multiplets. The blue (cyan) dashed line indicates the 2σ (3σ) range of the muon $g-2$ data. A gluino lower bound $m_{\tilde{g}} \gtrsim$ 1.5 TeV is shown in the figure.

(iii) light sbottom mass $m_{\tilde{b}_1} \gtrsim 0.84$ TeV,

(iv) first two generation squarks $m_{\tilde{q}} \gtrsim 1.0 \sim 1.4$TeV.

From the numerical results, we have the following observations:

(i) Scenario A: Fig. 1 shows the scan results of scenario A in which the Δa_μ versus $m_{\tilde{g}}$ plots with complete GUT multiplets are given. The blue (cyan) dashed line indicates the 2σ (3σ) range of $g_\mu - 2$ data. All surviving points satisfy the constraints (1-6) except the bounds from the dark matter relic density and the gluino mass. The most stringent constraints come from the LHC bounds on gluino mass, which excluded a great majority of the survived points that solve the $g_\mu - 2$ anomaly at 2σ level. As the messenger species number N gets larger, more and more points can survive the gluino mass bound.

The gluino is upper bounded by about 2.5 TeV (2.0 TeV) if the $g_\mu - 2$ anomaly is solved at 3σ (2σ) level. We know that the $g_\mu - 2$ anomaly can be solved if the relevant sparticles $\tilde{\mu}$, $\tilde{\nu}_\mu$, $\tilde{B}$, $\tilde{W}$ are lighter than 600–700 GeV [5] (the region with a smaller $\tan\beta$ needs even lighter sparticles). In AMSB, the whole low energy spectrum is determined by the value of F_ϕ. So, in order to solve the $g_\mu - 2$ anomaly, the mass scale of $\tilde{\mu}$, $\tilde{\nu}_\mu$, $\tilde{B}$, $\tilde{W}$ determines the upper bound of F_ϕ, which, on the other hand, sets a bound on gluino mass. The allowed range of F_ϕ versus the messenger scale $M_{\rm mess}$ in scenario A is shown in the left panel of Fig. 2. It is obvious from the plots that the scale of F_ϕ is indeed upper bounded to account for the $g_\mu - 2$ anomaly. We should note that the deflection of the RGE trajectory and the messenger-matter

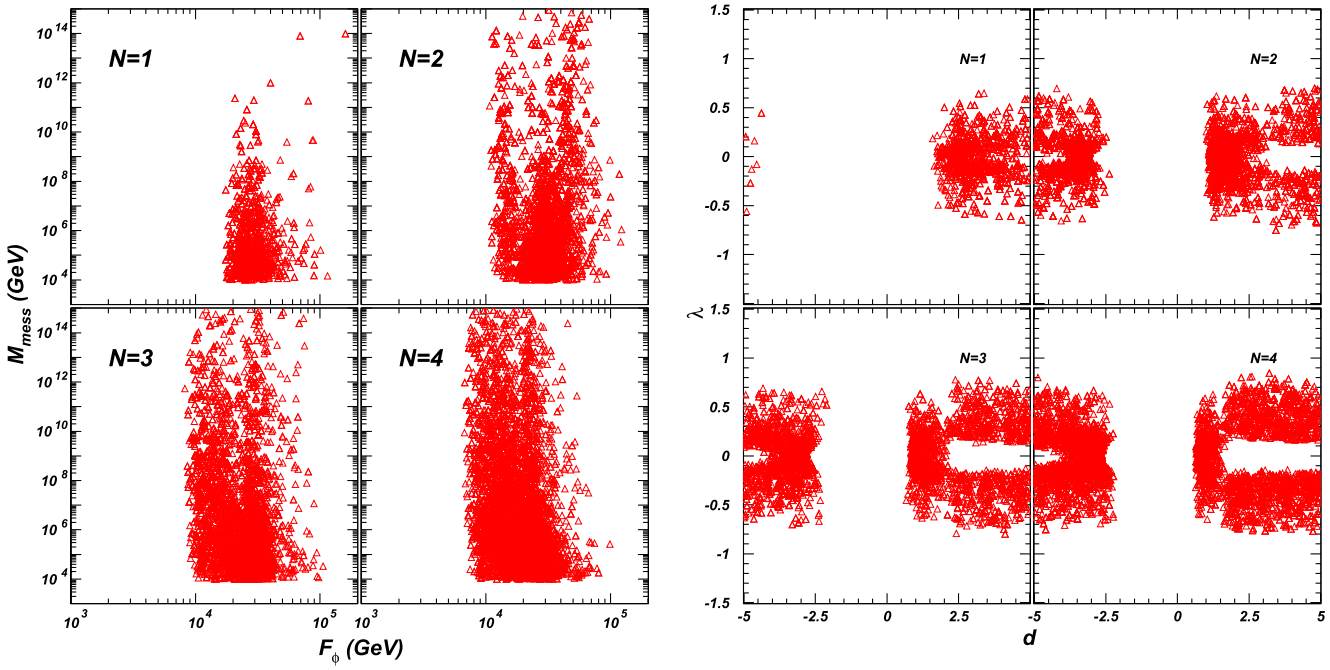

FIG. 2. Same as Fig. 1, but showing the value of F_ϕ versus the messenger scale $M_{\rm mess}$ (the left panel) and the deflection parameter d versus the messenger-matter couplings $\lambda \equiv \lambda_E$ (the right panel).

TABLE I. The range of d within which the wino is lighter than the bino for various messenger species N in scenario A.

	$N=1$	$N=2$	$N=3$	$N=4$
d	$-4.6 < d < 2.86$	$-2.3 < d < 1.43$	$-1.53 < d < 0.95$	$-1.15 < d < 0.72$

interactions can loosen the bound of F_ϕ in comparison with the ordinary AMSB.

The deflection parameter d versus the messenger-matter couplings $\lambda_E \equiv \lambda$ is plotted in the right panel of Fig. 2. We see that additional messenger-matter interactions are welcome to explain the $g_\mu - 2$ anomaly. Only a small range of d is allowed without leptonic messenger-matter interactions ($\lambda_E = 0$). However, the allowed range for d enlarges with nontrivial messenger-matter interactions.

Our numerical results indicate that the majority part of the allowed parameter space cannot satisfy the upper bound of dark matter relic density. This result can be understood from the hierarchies among the gauginos at the EW scale. From Eq. (2.64), the gaugino mass ratios at the weak scale are given by

$$M_1 : M_2 : M_3 \approx [6.6 - d(\Delta b_1)] : 2[1 - d(\Delta b_2)] : 6[-3 - d(\Delta b_3)]. \tag{3.8}$$

Knowing the range of the deflection parameter d, the lightest gaugino can be identified.

It can be seen in case $N = 1$ that the deflection parameter d is lower bounded to $d \gtrsim 1.5$ for a positive d while $d \lesssim -4.5$ for a negative d. From Eq. (3.8) we can see that for $-4.6 < d < 2.8$ the lightest gaugino will be the wino; otherwise the lightest gaugino will be the bino. It is well known that the relic density constraints for binolike dark matter are very stringent and possible coannihilation with sleptons or resonance is needed to obtain the correct DM relic density. So in a majority of the parameter space allowed by $g_\mu - 2$ and the gluino mass bound, the LSP is binolike and can hardly give the right DM relic density. On the other hand, a small portion of the allowed parameter space predicts a winolike LSP that leads to insufficient dark matter abundance for a wino mass below 3 TeV unless other DM components (for example, axion) are present. Heavy winolike LSP of order 3 TeV always leads to a heavy bino and sleptons which otherwise cannot explain the $g_\mu - 2$ anomaly. Given the upper bounds on F_ϕ from $g_\mu - 2$ and gluino mass, the wino is always much lighter than 3 TeV. We give in Table I the range of d, within which the wino is lighter than the bino for various messenger species N. We can see that only a small portion of parameter space with a positive d can satisfy the dark matter relic density upper bound. The vast parameter space with a binolike LSP is stringently constrained by a dark matter relic density upper bound. We checked that a very small region can satisfy such relic density constraints. So generalized deflected AMSB scenarios with complete GUT representation of messengers are not favored in solving the $g_\mu - 2$ discrepancy.

We should note that the constraints from the gluino can be alleviated if we introduce pure colored messenger particles [without $SU(2)_L$ and $U(1)_Y$ quantum numbers]. We can see from the expressions for the soft SUSY parameters that the value of Δb_3 can essentially control the gluino mass. More pure colored messenger particles always mean a heavy gluino for a positive deflection parameter, which, on the other hand, may spoil the gauge coupling unification. As noted in the previous section, the complete representation messengers may seem incomplete at the low energy X threshold. However, the perturbative gauge coupling unification may be spoiled with more additional messenger species. We discuss the detailed consequence of general messenger sectors versus gauge coupling unification in our subsequent studies.

(ii) Scenario B:

The scatter plots of the surviving samples showing a_μ versus $m_{\tilde{g}}$ in scenario B are shown in Fig. 3, in which the upper panel is for scenario B1 and the lower panel is for scenario B2. We can see that a lot of points that can fully account for the $g_\mu - 2$ anomaly can survive the LHC gluino mass bound, especially, for a larger M. So scenarios with the incomplete GUT representation of messengers are more favored by the $g_\mu - 2$ data.

Similar to scenario A, the upper bound of gluino mass can be understood from the upper bound of F_ϕ, which is obvious in Fig. 4 for both cases. The upper mass bound of the gluino is around 3 TeV (2.7 TeV) in both scenarios if the muon $g-2$ is explained at the 3σ (2σ) level. Such a light gluino will be accessible at future LHC experiments.

The deflection parameter d versus the messenger-matter couplings $\lambda_E \equiv \lambda$ in scenario B is plotted in Fig. 5 with all points satisfying both the upper and

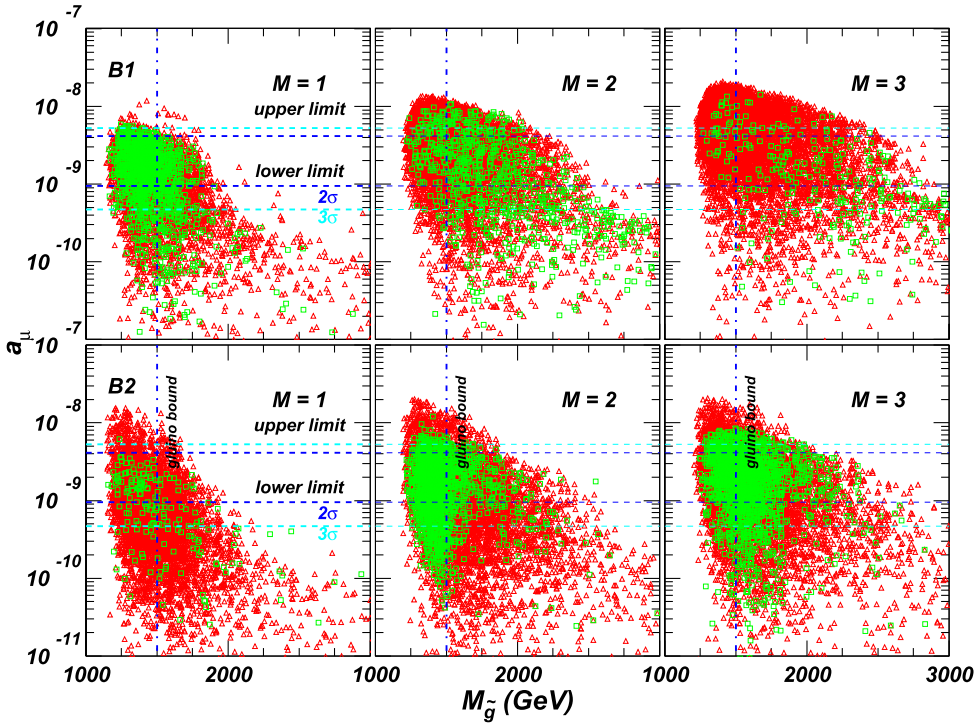

FIG. 3. The scatter plots of the surviving samples showing the muon $g-2$ versus the gluino mass in scenario B with incomplete GUT multiplets (adjoint messengers). The upper panel corresponds to scenario B1 while the lower panel is for scenario B2. The green □ samples satisfy both the upper and lower bounds of the dark matter relic density.

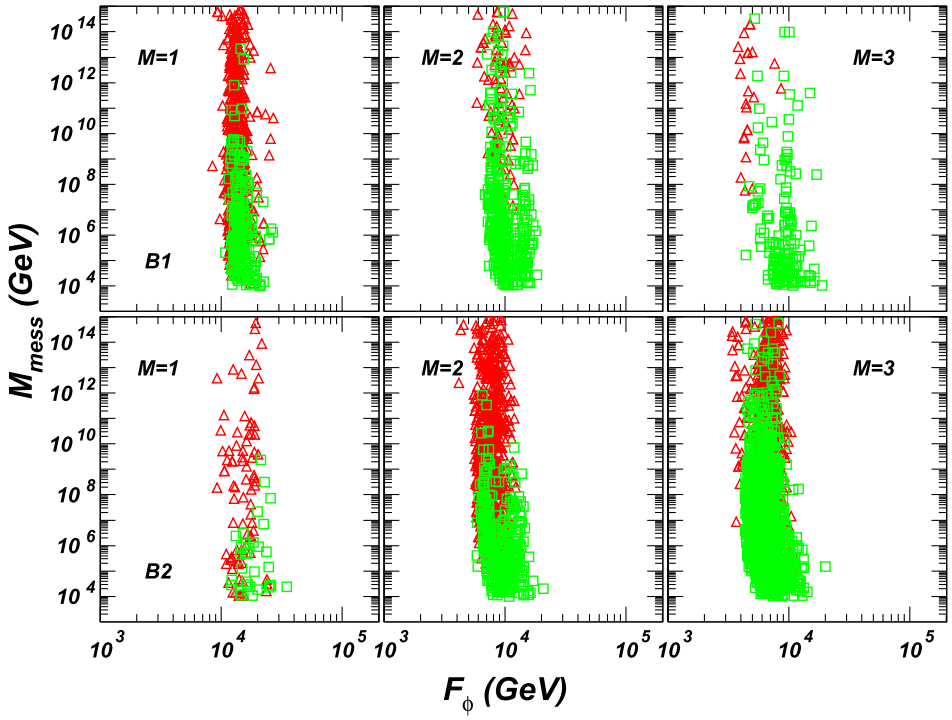

FIG. 4. Scatter plots showing F_ϕ versus the messenger scale $M_{\rm mess}$ for scenario B. All the points satisfy both the lower and upper bounds of dark matter relic density and collider constraints. The red △ (green □) samples are excluded (allowed) by the gluino mass bound $m_{\tilde{g}} \geq 1.5$ TeV.

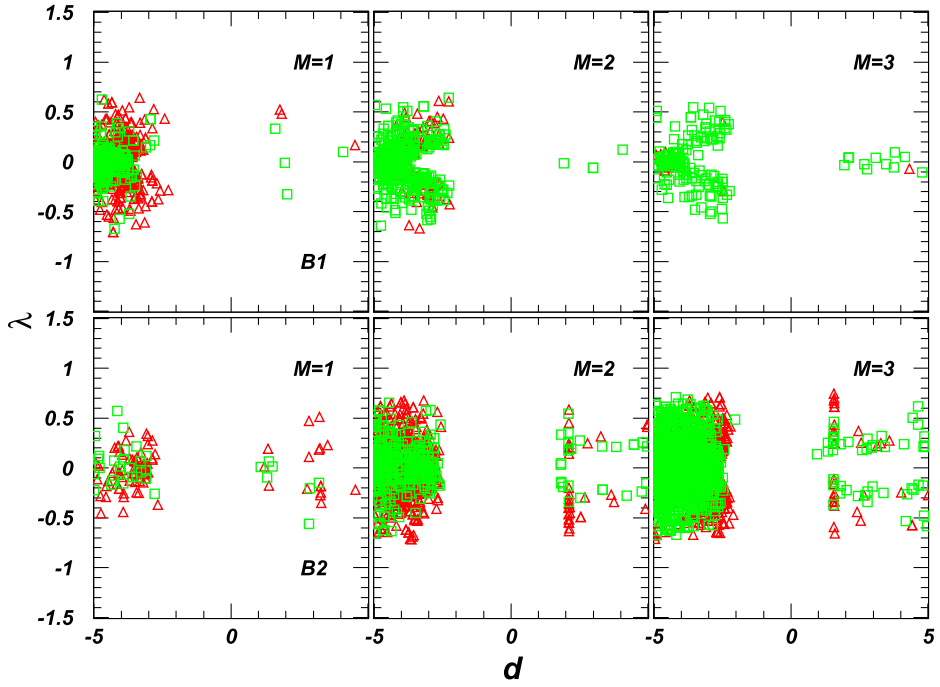

FIG. 5. Same as Fig. 4, but showing the deflection parameter d versus the messenger-matter couplings λ_E.

lower bound of DM relic density. Again, additional nontrivial messenger-matter interactions are obviously advantageous in solving the $g_\mu - 2$ anomaly with which the allowed range for d enlarges. Besides, the nonvanishing messenger-matter interactions $\lambda \neq 0$ can be used to solve the $g_\mu - 2$ anomaly for a relatively small deflection parameter d, especially for the scenario B1. We can see from Fig. 5 that in scenario B1 the maximum negative d is -3.5 with $\lambda = 0$. However, the maximum negative d changes to almost -2 with nonvanishing messenger-matter interactions. A small deflection parameter $|d|$ is relatively easy for model buildings. In scenario B2, it is not possible to solve the $g_\mu - 2$ anomaly with $\lambda = 0$ for a positive d. With messenger-matter interactions, a positive deflection parameter also works.

In Fig. 5 the survived points that satisfy both the upper and lower bounds of dark matter relic density are shown as green □. The numerical calculation indicates that the number of points that satisfy the dark matter relic density decreases with M in scenario B1, but increases with M in scenario B2. This can be understood from the mass ratio between the bino and the gluino with (the most favorite) large negative deflection parameter $d \sim -4$. For a gluino mass between 1.5 and 3 TeV, the mass ratio should be adjusted to a proper value at $M_3 : M_1 \sim \mathcal{O}(10)$ to fully account for the dark matter relic density by decreasing (scenario B1) or increasing (scenario B2) the value of M. The bino dominated neutralino often leads to overabundance of DM, unless (co)annihilation processes reduce the relic density to levels compatible with Planck.

We should note that some portion of the parameter space with insufficient DM relic abundance is not displayed in Figs. 4 and 5. Following the discussions in scenario A, we obtain Table II from Eq. (3.8), showing the range of the deflection parameter d within which the wino is lighter than the bino. Constrained by F_ϕ, a light winolike DM always leads to insufficient relic abundance.

The DM SI direct detection constraints from LUX and PandaX are shown in Fig. 6. It can be seen that a large portion of points that satisfy the DM relic density can survive the SI direct detection constraints. We know that interactions between the bino DM and the nucleons are primarily mediated by the

TABLE II. The range of d within which the wino is lighter than the bino for various messenger species M in scenario B.

		$M=1$	$M=2$	$M=3$
Scenario B1	d	$-0.92 \lesssim d \lesssim 1.23$	$-0.51 \lesssim d \lesssim 0.78$	$-0.35 \lesssim d \lesssim 0.95$
Scenario B2	d	$-1.21 \lesssim d \lesssim 1.05$	$-0.69 \lesssim d \lesssim 0.64$	$-0.49 \lesssim d \lesssim 0.46$

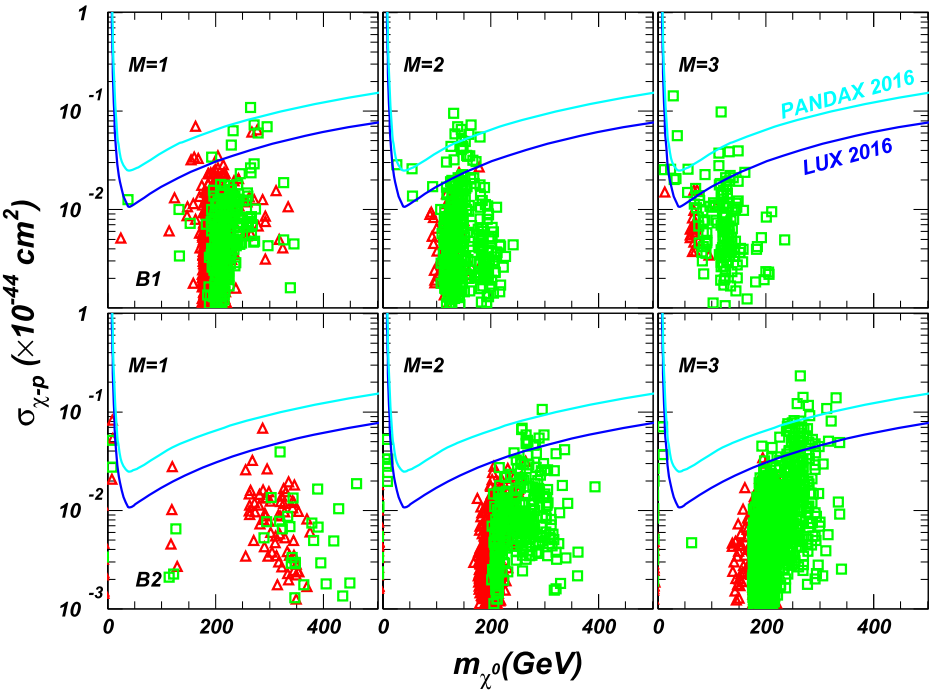

FIG. 6. Same as Fig. 4, but showing the spin-independent DM direct detection constraints from LUX 2016 and PandaX.

t-channel scalar Higgs bosons (h_0 and H_0), or by s-channel squarks (with the t-channel Z-boson exchange process highly suppressed). As the squarks are not found at the LHC, their masses should be significantly larger than the Higgs masses. So the SI cross section is dominated by the Higgs-mediated process, despite the associated suppression by Yukawa couplings and the small Higgsino fraction. In scenario B, the type of the neutralino that can give the right DM relic abundance is almost binolike with a small Higgsino component, thus suppressing the SI direct detection cross sections.

IV. CONCLUSIONS

We proposed to introduce general messenger-matter interactions in the deflected anomaly mediated SUSY breaking scenario to explain the $g_\mu - 2$ anomaly. Scenarios with complete or incomplete GUT multiplet messengers are discussed, respectively. The introduction of incomplete GUT mulitiplets can be advantageous in various aspects. We found that the $g_\mu - 2$ anomaly can be solved in both scenarios under current constraints including the gluino mass bounds, while the scenarios with incomplete GUT representation messengers are more favored by the $g_\mu - 2$ data. We also found that the gluino is upper bounded by about 2.5 TeV (2.0 TeV) in scenario A and 3.0 TeV (2.7 TeV) in scenario B if the generalized deflected AMSB scenarios are used to fully account for the $g_\mu - 2$ anomaly at 3σ (2σ) level. Such a gluino should be accessible in the future LHC searches. Dark matter constraints, including DM relic density and direct detection bounds, favor scenario B with incomplete GUT multiplets. Much of the allowed parameter space for scenario B could be covered by the future DM direct detection experiments.

ACKNOWLEDGMENTS

This work was supported by the Natural Science Foundation of China under Grants No. 11375001, No. 11675147, and No. 11675242, by the Open Project Program of State Key Laboratory of Theoretical Physics, ITP, CAS (Grant No. Y5KF121CJ1), by the Innovation Talent project of Henan Province under Grant No. 15HASTIT017 and the Young-Talent Foundation of Zhengzhou University, by the CAS Center for Excellence in Particle Physics (CCEPP), and by the CAS Key Research Program of Frontier Sciences.

[1] G. Aad *et al.* (ATLAS Collaboration), Phys. Lett. B **710**, 49 (2012).
[2] S. Chatrachyan *et al.* (CMS Collaboration), Phys. Lett. B **710**, 26 (2012).
[3] The ATLAS Collaboration, Report No. ATLAS-CONF-2016-052.
[4] The ATLAS Collaboration, Report No. ATLAS-CONF-2016-050.
[5] M. Byrne, C. Kolda, and J. E. Lennon, Phys. Rev. D **67**, 075004 (2003).
[6] A. H. Chamseddine, R. L. Arnowitt, and P. Nath, Phys. Rev. Lett. **49**, 970 (1982); H. P. Nilles, Phys. Lett. **115B**, 193 (1982); L. E. Ibanez, Phys. Lett. **118B**, 73 (1982); R. Barbieri, S. Ferrara, and C. A. Savoy, Phys. Lett. **119B**, 343 (1982); H. P. Nilles, M. Srednicki, and D. Wyler, Phys. Lett. **120B**, 346 (1983); J. R. Ellis, D. V. Nanopoulos, and K. Tamvakis, Phys. Lett. **121B**, 123 (1983); J. R. Ellis, J. S. Hagelin, D. V. Nanopoulos, and K. Tamvakis, Phys. Lett. **125B**, 275 (1983); N. Ohta, Prog. Theor. Phys. **70**, 542 (1983); L. J. Hall, J. D. Lykken, and S. Weinberg, Phys. Rev. D **27**, 2359 (1983).
[7] M. Dine, W. Fischler, and M. Srednicki, Nucl. Phys. **B189**, 575 (1981); S. Dimopoulos and S. Raby, Nucl. Phys. **B192**, 353 (1981); M. Dine and W. Fischler, Phys. Lett. **110B**, 227 (1982); M. Dine and A. E. Nelson, Phys. Rev. D **48**, 1277 (1993); M. Dine, A. E. Nelson, and Y. Shirman, Phys. Rev. D **51**, 1362 (1995); M. Dine, A. E. Nelson, Y. Nir, and Y. Shirman, Phys. Rev. D **53**, 2658 (1996); G. F. Giudice and R. Rattazzi, Phys. Rep. **322**, 419 (1999).
[8] L. Randall and R. Sundrum, Nucl. Phys. **B557**, 79 (1999); G. F. Giudice, M. A. Luty, H. Murayama, and R. Rattazzi, J. High Energy Phys. 12 (1998) 027.
[9] I. Jack and D. R. T. Jones, Phys. Lett. B **465**, 148 (1999).
[10] I. Jack and D. R. T. Jones, Phys. Lett. B **482**, 167 (2000); E. Katz, Y. Shadmi, and Y. Shirman, J. High Energy Phys. 08 (1999) 015; N. ArkaniHamed, D. E. Kaplan, H. Murayama, and Y. Nomura, J. High Energy Phys. 02 (2001) 041; R. Sundrum, Phys. Rev. D **71**, 085003 (2005); K. Hsieh and M. A. Luty, J. High Energy Phys. 06 (2007) 062; Y. Cai and M. A. Luty, J. High Energy Phys. 12 (2010) 037; T. Kobayashi, Y. Nakai, and M. Sakai, J. High Energy Phys. 06 (2011) 039.
[11] A. Pomarol and R. Rattazzi, J. High Energy Phys. 05 (1999) 013; R. Rattazzi, A. Strumia, and J. D. Wells, Nucl. Phys. **B576**, 3 (2000).
[12] N. Okada, Phys. Rev. D **65**, 115009 (2002); N. Okada and H. M. Tran, Phys. Rev. D **87**, 035024 (2013).
[13] A. E. Nelson and N. J. Weiner, arXiv:0210288.
[14] K. Hsieh and M. A. Luty, J. High Energy Phys. 06 (2007) 062.
[15] M. Luty and R. Sundrum, Phys. Rev. D **67**, 045007 (2003).
[16] L. L. Everett, I. W. Kim, P. Ouyang, and K. M. Zurek, Phys. Rev. Lett. **101**, 101803 (2008).
[17] F. Wang, Phys. Lett. B **751**, 402 (2015).
[18] T. Han, T. Yanagida, and R. J. Zhang, Phys. Rev. D **58**, 095011 (1998).
[19] I. Gogoladze, A. Mustafayev, Q. Shafi, and C. S. Un, Phys. Rev. D **94**, 075012 (2016); I. Gogoladze and C. S. Un, Phys. Rev. D **95**, 035028 (2017).
[20] L. Calibbi, T. Li, A. Mustafayev, and S. Raza, Phys. Rev. D **93**, 115018 (2016).
[21] F. Wang, W. Wang, J. M. Yang, and Y. Zhang, J. High Energy Phys. 07 (2015) 138.
[22] G. F. Giudice and R. Rattazzi, Nucl. Phys. **B511**, 25 (1998).
[23] G. F. Giudice and R. Rattazzi, Phys. Rep. **322**, 419 (1999).
[24] J. A. Evans and D. Shih, J. High Energy Phys. 08 (2013) 093.
[25] Z. Chacko and E. Ponton, Phys. Rev. D **66**, 095004 (2002).
[26] For a comparative study of NMSSM and MSSM, see J. Cao, Z. Heng, J. M. Yang, Y. Zhang, and J. Zhu, J. High Energy Phys. 03 (2012) 086.
[27] Y. Cai and M. A. Luty, J. High Energy Phys. 12 (2010) 037.
[28] Muon G-2 Collaboration, Phys. Rev. D **73**, 072003 (2006); Muon G-2 Collaboration, Phys. Rev. D **80**, 052008 (2009); B. L. Roberts, Chin. Phys. C **34**, 741 (2010).
[29] M. Davier, A. Hoecker, B. Malaescu, C. Z. Yuan, and Z. Zhang, Eur. Phys. J. C **66**, 1 (2010); K. Hagiwara, R. Liao, A. D. Martin, D. Nomura, and T. Teubner, J. Phys. G **38**, 085003 (2011); M. Davier, A. Hoecker, B. Malaescu, and Z. Zhang, Eur. Phys. J. C **71**, 1 (2011); J. Prades, E. de Rafael, and A. Vainshtein, Adv. Ser. Dir. High Energy Phys. **20**, 303 (2009).
[30] M. Endo, K. Hamaguchi, S. Iwamoto, and K. Yanagi, J. High Energy Phys. 06 (2017) 031; M. Endo, K. Hamaguchi, T. Kitahara, and T. Yoshinaga, J. High Energy Phys. 11 (2013) 013; B. Zhu, R. Ding, and T. Li, Phys. Rev. D **96**, 035029 (2017); C. Li, B. Zhu, and T. Li, arXiv:1704.05584; M. Lindner, M. Platscher, and F. S. Queiroz, arXiv:1610.06587 [Rev. Phys. Rep. (to be published)]; A. Kobakhidze, M. Talia, and L. Wu, Phys. Rev. D **95**, 055023 (2017).
[31] S. Schael *et al.* (ALEPH and DELPHI and L3 and OPAL and SLD and LEP Electroweak Working Group and SLD Electroweak Group and SLD Heavy Flavour Group Collaborations), Phys. Rep. **427**, 257 (2006).
[32] P. A. R. Ade *et al.* (Planck Collaboration), Astron. Astrophys. **571**, A16 (2014).
[33] J. Dunkley *et al.* (WMAP Collaboration), Astrophys. J. Suppl. Ser. **180**, 306 (2009).
[34] D. S. Akerib *et al.*, Phys. Rev. Lett. **118**, 021303 (2017).
[35] C. Fu *et al.*, Phys. Rev. Lett. **118**, 071301 (2017).
[36] V. Khachatryan *et al.* (CMS and LHCb Collaborations), Nature (London) **522**, 68 (2015).
[37] Y. Amhis *et al.* [Heavy Flavor Averaging Group (HFAG)], arXiv:1412.7515.
[38] C. Patrignani *et al.* (Particle Data Group), Chin. Phys. C **40**, 100001 (2016).
[39] M. Aaboud *et al.* (ATLAS Collaboration), Eur. Phys. J. C **76**, 547 (2016); The CMS Collaboration, Report No. CMS-PAS-SUS-16-015;The ATLAS Collaboration, Report No. ATLAS-CONF-2016-078;CMS Collaboration, Report No. CMS-PAS-SUS-16-030.